Pramāna – J. Phys., Vol. 28, No. 5, May 1987, pp. 529–545. © Printed in India.

Transformation kinetics of A-15 superconductors formed by solid state reactions

A V NARLIKAR
National Physical Laboratory, Hillside Road, New Delhi 110012, India

Abstract. Various fabrication processes devised for making multifilamentary A-15 superconductors are all based on solid state reactions, transforming the host metal into the binary A-15 phase. The kinetics of the growth process involved in the compound formation form the theme of this paper.

Keywords. A-15 superconductors; Nb_3Sn; diffusion; grain boundaries; ordering.

PACS No. 74·50

1. Introduction

Phase transformation of bcc Nb into Nb_3Sn of A-15 crystal structure caused by solid state diffusion of Sn into Nb has led to several processing routes for fabricating Nb_3Sn in multifilamentary form. They include the conventional bronze process, in-situ and powder metallurgy techniques, the modified jelly roll process, etc. Actually, these processes are really no more than different ways of realizing composite conductors containing a large number of fine Nb filaments in a bronze matrix. Diffusion reactions at 550 to 800°C result in Nb_3Sn layers at the bronze-Nb interfaces (figure 1). V_3Ga and V_3Si are two other important binary A-15s of A_3B type produced in this way.

In any phase transformation one is confronted with two pertinent questions: (a) why does a particular phase change occur?, and (b) how does it occur? The answer to (a) requires thermodynamic considerations while that to (b) involves the kinetics. The thermodynamics of A-15 formation, described elsewhere (Dew-Hughes and Luhman 1978; Narlikar and Dew-Hughes 1985a, b) is considered outside the scope of the present paper.

Turning to kinetics, there are four types of kinetics associated with A-15 layer formation: (i) nucleation, (ii) grain growth, (iii) layer growth and (iv) ordering. Nucleation kinetics are of prime importance for compound formation. The critical current density J_c of the A-15 layer is controlled by grain growth kinetics. The overall critical current I_c is determined by layer growth kinetics. Finally, the critical temperature T_c depends sensitively on the long range order (LRO) of the compound layers, which in turn is determined by ordering kinetics. Interestingly, all the four processes come into operation almost simultaneously with the start of diffusion annealing.

In this paper we briefly describe the four kinds of kinetics. Although the kinetics story is basically independent of various fabrication routes referred above a greater emphasis is laid on the results obtained with bronze process. This is because its

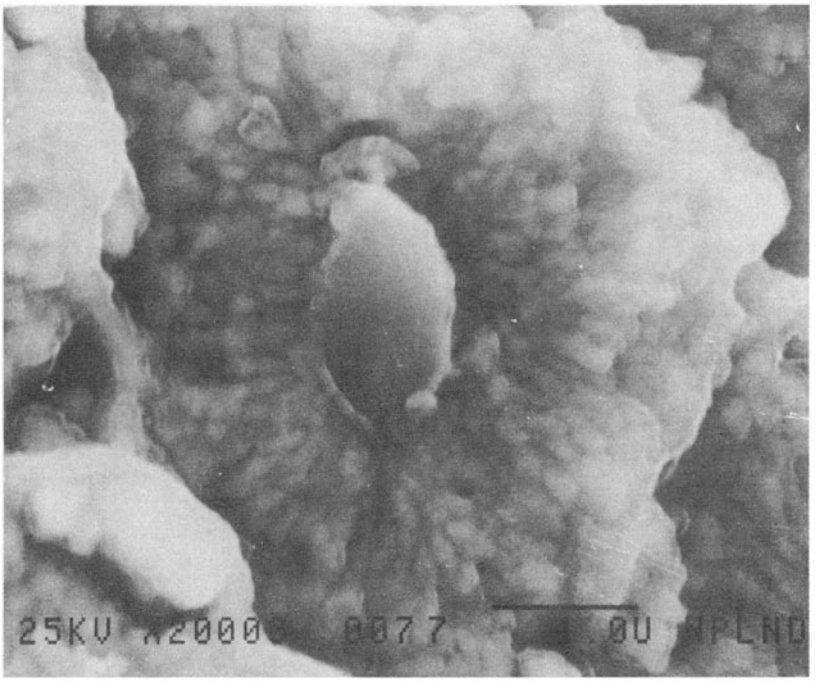

Figure 1. Scanning electron micrograph of Nb_3Sn layers formed at the bronze-Nb interfaces.

commercial viability is proven and there is an abundance of data on the bronze-processed samples.

2. Nucleation kinetics

The problem of nucleation of A-15 phase in a diffusion couple has received little attention so far. It is clear that the nuclei for the initial layer form at the bronze-Nb interface and for the subsequent layers at the Nb_3Sn-Nb interface. The driving force for nucleation must arise from two factors: (a) the free energy difference between the transformed (i.e. Nb_3Sn) and transforming phases (i.e. Nb), and (b) release of stored energy of heavily deformed Nb filaments by formation of strain free A-15 grains—a situation analogous to recrystallization. The negative contribution of volume energy ΔG_v favouring the formation of Nb_3Sn is countered by two positive contributions: (i) the surface energy ΔG_s associated with the creation of an interface between Nb and Nb_3Sn, and (ii) the volume contribution of strain energy ΔG_m caused by 37% of volume expansion when Nb is transformed to Nb_3Sn. The free energy change associated with the formation of Nb_3Sn particle of radius r is given by,

$$\Delta G = -A_1 r^3 + A_2 r^2, \tag{1}$$

where A_1 and A_2 are constants and ΔG_m is considered simply to modify ΔG_v. For a particle of small radius the positive surface energy term dominates whereas when the radius exceeds a certain critical value r_0 the overall free energy becomes negative and

the transformation to the new phase is favoured (figure 2). E_0 in the figure represents the nucleation barrier.

As Nb_3Sn has a crystal structure and the lattice parameter both considerably differing from Nb its nucleation will be heterogeneous. Nuclei formed at a lower reaction temperature are expected to be more Sn-deficient than those formed at a higher temperature and in regard to the lattice parameter they would be relatively closer to Nb. Thus, a lower reaction temperature would favour smaller nuclei more closely spaced, while the situation will be just opposite at higher temperatures. Thus, the initial grain size of A-15 layers formed at a lower reaction temperature would be smaller than that formed at a higher temperature. This is corroborated experimentally (Okuda *et al* 1983) and it holds relevance to the layer growth kinetics.

Junction points of grain boundaries and dislocation cell walls in Nb filaments are expected to provide the favoured sites for A-15 nucleation. Finer Nb filaments formed by heavy reductions would have large number of closely spaced nucleation sites, leading to smaller A-15 grains as reported by Okuda *et al* (1983).

Growth of Nb_3Sn nuclei would occur by migration of Nb_3Sn-Nb boundaries towards Nb. If there are N nucleation sites per unit volume along the reaction interface, for spherical nuclei growing with a velocity u, the volume fraction transformed $V(t)$ after a time t is given by Cahn and Hagel (1962),

$$V(t) = 1 - \exp(-\tfrac{4}{3}\pi N(ut)^3), \tag{2}$$

where $u = C\exp(-U_m/kT)$. The growth of the nuclei is due to thermally activated transfer of atoms from one crystal to another across a moving interface. The parameter C in the above equation includes the chemical potential difference between the final (i.e. Nb_3Sn) and the initial (i.e. Nb) phases which provide the driving force for boundary migration. This process would continue until the neighbouring grains of Nb_3Sn have a

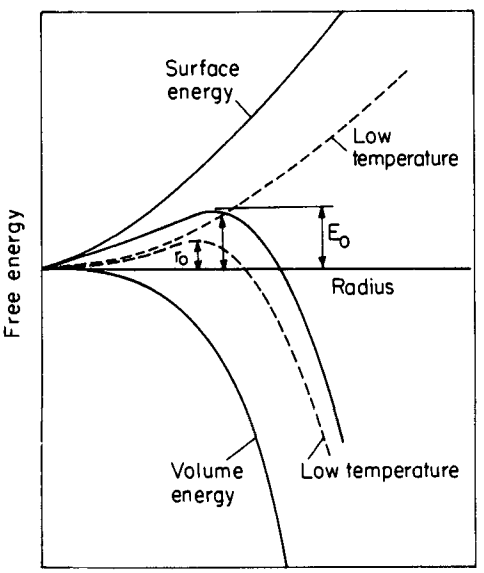

Figure 2. Energies involved in A-15 phase nucleation.

common grain boundary. Thereafter, grain growth in the conventional sense occurring in fully recrystallized metal will follow.

3. Grain growth kinetics

When the grain structure is free from variations in stored energy and possesses the same phase throughout, the driving force for grain growth stems from decrease in the free energy resulting from reduction in the grain boundary area. Since the grain diameters of A-15 layers tend to be rather small, reliable data of their growth kinetics are still lacking. Theory of grain growth in metallic systems applies to the ideal situation of the behaviour of cells in a soap froth which grow or shrink at the expense of each other so as to reduce the total boundary area. This gives a parabolic cell growth of the form,

$$d_t^2 - d_0^2 = K't, \tag{3}$$

where d_0 is the initial grain diameter and d_t after a time t. Boundaries advance to their centres of curvature by thermally activated process with activation energy U, and (3) becomes,

$$d_t^2 - d_0^2 = K_0 \exp[-U/kT]t. \tag{4}$$

This holds also for A-15 grains formed by solid state reactions. The available information on A-15s is summarized below.

(i) Effect of melting and reaction temperatures: Larger the melting temperature smaller is the grain growth at a fixed reaction temperature. Nb_3Sn, V_3Si and V_3Ga possess melting temperatures of 2100, 1900 and 1300°C respectively and of these V_3Ga exhibits the largest and Nb_3Sn the smallest grain growth and grain sizes (Livingston 1977).

(ii) Effect of cold-work: More heavily cold worked filaments give rise to smaller A-15 grains after diffusion reactions.

(iii) Addition of impurities: Adding impurities to diffusion couple can affect the grain size in two ways: (a) layer growth is enhanced and thus a lesser time is available for grains to grow, and (b) grain boundaries get pinned by impurities. Addition of impurities like Al, Zn, or Mg to the bronze matrix and Ti, Zr or Hf to filaments enhances the layer growth and the grain size is found to be smaller.

(iv) Grain size distribution: The grains closer to the bronze interface are formed prior to the inner grains and hence there is a radical decrease in the grain size towards the filament centre (figure 3).

(v) Grain morphology: A majority of our findings indicate that a faster layer growth occurring at higher temperatures produces equiaxed grains, while at lower temperatures the grains formed tend to be columnar. According to Okuda *et al* (1983) an enhanced delivery of Sn atoms to the reaction interface makes nucleation of new grains favourable. When transportation of Sn atoms is slow the atoms attach themselves to the existing grains making them columnar. The grains at Nb_3Sn-Nb interface are columnar while in the middle and outer regions of the layer they are generally equiaxed (figure 4). Cave and Weir (1983) attributed this to 37% of volume expansion associated with Nb_3Sn formation which pushes the reaction interface outwards. The strain

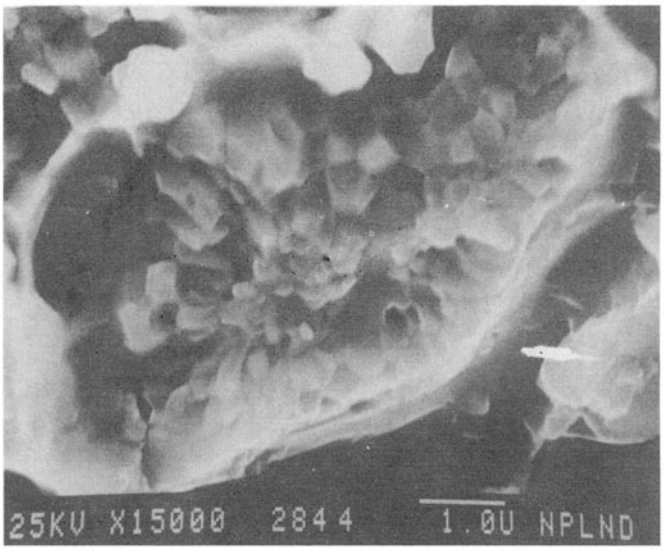

Figure 3. Grains in fully reacted Nb_3Sn layer.

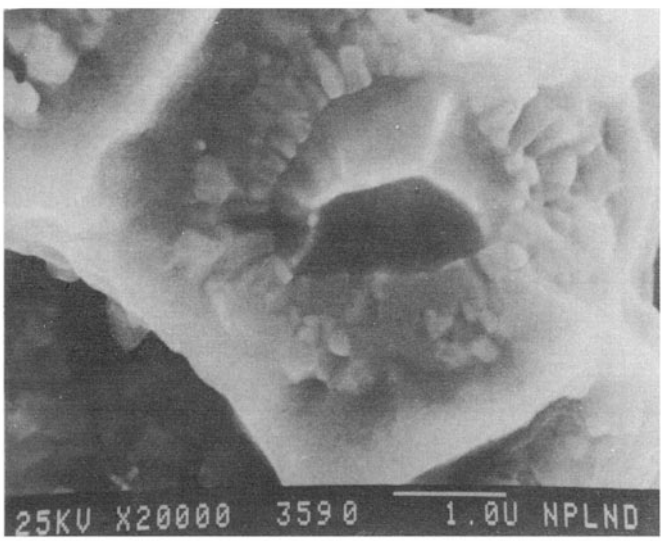

Figure 4. Columnar grains at Nb_3Sn-Nb interface.

relaxation does not take place through creation of cracks but by a different process that creates dislocations to separate off the tips of the columnar grains which subsequently relax by rotation and sliding.

4. Growth laws

Thickness of the A-15 layer of Nb_3Sn and V_3Ga formed in bronze-processed samples has been extensively studied at the National Physical Laboratory (NPL) and elsewhere

as a function of various process parameters such as diffusion temperature, reaction time and concentration of *B* element (i.e., Sn or Ga) in copper matrix etc., and as a rule the growth is found to be controlled by the general equation:

$$R = kt^n, \tag{5}$$

where R is the layer thickness formed at a fixed reaction temperature after a time t, n is the numerical time exponent, and k is the reaction rate constant. The parameter k, as will be seen later, is related to the diffusivity of *B* element relevant to the pertinent rate-controlling step responsible for the layer growth and also depends upon various process parameters.

Growth is parabolic, subparabolic or superparabolic respectively when n is equal to, less than or more than 0·5. Interestingly, diffusion couples composed of the same components are found to yield all the three growth laws under different situations. In fact, as may be seen from table 1, the observed time exponents vary in a wide range from 0·15 to 1·0. Further, k and n respond in an intriguing way to the process conditions; the enhanced growth rate stems sometimes from increase in k and sometimes from increase in n. For Nb_3Sn, in multifilamentary composites the growth is invariably subparabolic while in the monofilamentary situation it is either parabolic or superparabolic. V_3Ga, on the other hand, shows mostly parabolic growth.

Results reported in a recent literature survey (Narlikar and Dew-Hughes 1985b) of layer growth studies seem diverse and conflicting. Growth models, compatible with the general principles of solid state diffusion and physical metallurgy, must correctly predict reported growth rates and the whole range of n values observed under different process conditions. The relevance of such model calculations in sorting out the anomalies is obvious.

Reddi *et al* (1978) and Agarwal *et al* (1984) have developed growth kinetic models which provide a starting point to understand various features of the compound layer

Table 1. Effect of impurities on layer growth kinetics (Narlikar and Dew-Hughes 1985a).

Matrix	Core	Grain size/ grain growth	Layer growth	n
Cu-6%Sn-0·5%Mg	Nb	Reduced	Increased	0·5
Cu-7%Sn-0·9%Mg	Nb	-do-	-do-	0·5
Cu-5%Sn-4%Ga	Nb	-do-	-do-	0·5
Cu-7%Sn-1·5%Ti	Nb	-do-	-do-	0·58
Cu-6%Sn-4%Al	Nb-1%Al	-do-	-do-	0·58–0·71
Cu-(2%to10%Sn)	Nb	-do-		0·55–0·9
Cu-10%Sn	Nb-1%U	-do-		1·0
Cu-12%Sn	Nb	-do-	-do-	0·26–0·48
Cu-14%Sn	Nb	-do-	-do-	0·17
Cu-12%Sn	Nb	-do-	-do-	0·30
Cu-17·5%Ga	V-6·5%Ga	-do-	-do-	0·5
Cu-8%Ga	V-2%Ti	-do-	-do-	0·5
Cu-19%Ga-0·5%Mg	V-6%Ga	-do-	-do-	0·5
Cu-18%Ga	V	Increased	Decreased	0·35

formation. Some salient features of these models are consolidated in the following section.

5. Analytical models

Consider a three-component system: the pure Nb core, growing Nb_3Sn layer and Cu-Sn matrix. The growth of the compound layer occurs by diffusion of Sn from bronze through the existing layer of Nb_3Sn and the reaction takes place at the Nb_3Sn-Nb interface. The rate of layer growth will depend upon three rate-controlling steps, namely, the rate at which (i) Sn is supplied from bronze matrix to bronze-Nb_3Sn interface, (ii) Sn is transported across the Nb_3Sn layer to the Nb_3Sn-Nb interface, and (iii) Sn reacts with Nb to produce Nb_3Sn. If these processes proceed at different rates, the rate of layer growth will be controlled by whichever of them is the slowest. (iii) is the fastest, being almost instantaneous and, consequently, it is the slowness of (i) and (ii) that turns out to be the rate-controlling step. The models consider the two situations separately and predict various growth laws as summarized below.

5.1 *Growth controlled by diffusion through bronze matrix*

Various concentration profiles of the B element (Sn) in the composite are as shown in figure 5. The following parameters appear in the calculation: r_c, composite radius; r_F, initial radius of the filament; r', radius of the unreacted filament after a time t of diffusion reaction; C_i, initial concentration of the B element in the matrix, expressed as number of B atoms per unit volume; $C_{\alpha\beta}$, interface concentration of B in the matrix in equilibrium with the reacted compound β; $C_{\beta\alpha}$, interface concentration of B in the layer in equilibrium with the matrix α; $C_{\beta F}$, concentration of B in the layer at the β-F interface.

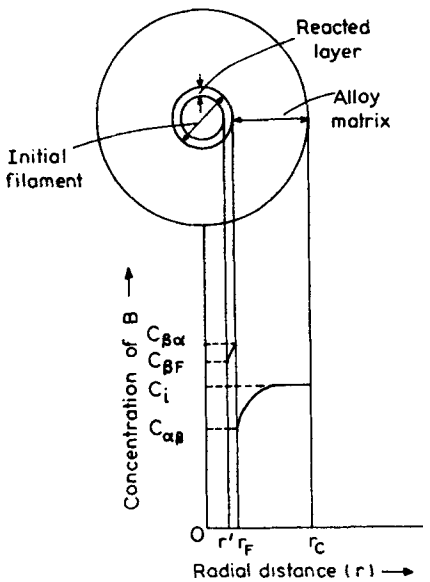

Figure 5. Various concentration profiles in the composite (after Reddi *et al* 1978).

Since the thickness of the reacted layer R is small compared to r_F, the concentration profile within the reacted layer can be assumed to be linear, giving the mean concentration of B in the reacted layer to be

$$\bar{C}_\beta = (C_{\beta\alpha} + C_{\beta F})/2.$$

As the layer growth is controlled by diffusion of B through the α-matrix, the flux at the α-β interface determines the overall kinetics. In this situation the models developed lead to three possibilities described below.

5.1a *Small depletion distance*: Depletion distance refers to the distance in the bronze matrix measured from α-β interface over which the Sn concentration drops from C_i to $C_{\alpha\beta}$. Small depletion distance leads to a parabolic growth,

$$R = k_1 t^{1/2}, \tag{6}$$

with rate constant,

$$k_1 = (D_\alpha^{1/2}/\bar{C}_\beta)\,(C_i - C_{\alpha\beta}), \tag{7}$$

where D_α is the diffusivity of B in α-matrix.

5.1b *Large depletion distance*: The growth law predicted is of the form

$$R = k_2 t^{2/3}, \tag{8}$$

with

$$k_2 = \frac{3D_\alpha^{2/3}}{2\bar{C}_\beta (9r_F)^{1/3}}(C_i - C_{\alpha\beta}). \tag{9}$$

5.1c *Depletion distance exceeding thickness of α-matrix*: The predicted growth is linear,

$$R = k_3 t, \tag{10}$$

with

$$k_3 = (D_\alpha/\bar{C}_\beta)k_0, \tag{11}$$

where k_0 is related to the concentration difference between the outer rim and α-β interface.

When C_i is large or when t is small, the effective diffusion distance is small and the growth predicted is parabolic. For small C_i and large t, n is expected to increase from 0·5 to 0·67. Results of Suenaga *et al* (1974), Dew-Hughes *et al* (1976), Luhman and Suenaga (1977) and Dew-Hughes and Suenaga (1978) obtained for monofilamentary Nb_3Sn all substantiate this contention. After prolonged diffusion, when the Sn-concentration at the outer rim starts depleting, the time exponent approaches 1·0. Increase in n with decrease in C_i, predicted by the model, was confirmed for Nb_3Sn by Reddi *et al* (1983) who found $n = 0{\cdot}9$ for the lowest value of C_i (figure 6).

When the growth is superparabolic and the growth rate is increased by the addition of impurities in the matrix or in the core, the obvious explanation of this from (8) is the increase in D_α. Addition of about 2% of Ti or Zr to V cores is found to significantly enhance Ga diffusion rate in the matrix, as confined by the formation of a large number

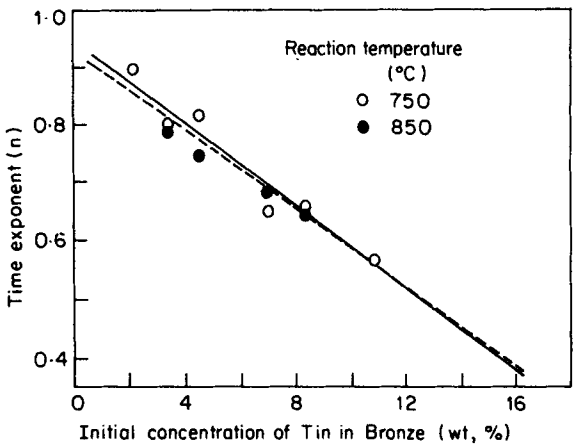

Figure 6. Increase in n with decrease in Sn-content in bronze (after Reddi *et al* 1983).

of Kirkendall voids at the α-β interface and the growth as reported by Berthel *et al* (1978) and Suenaga (1981) is superparabolic. Similarly, the addition of Al and Zn to the bronze enhances the growth rate of Nb_3Sn, as shown by Dew-Hughes *et al* (1976) and Wada *et al* (1978). Al and Zn in bronze are expected to enhance the vacancy concentration and thereby D_α is increased, giving rise to a higher reaction rate constant.

5.2 *Growth controlled by diffusion through layer*

We examine two possibilities: (a) bulk diffusion through the compound layer; (b) grain boundary diffusion through the compound layer: Here there are two situations to be considered: (i) zero grain growth; (ii) grain growth when (a) initial grain size is small and (b) initial grain size is large.

5.2a *Growth controlled by bulk diffusion through the layer*: The bulk diffusion tends to dominate over the grain boundary diffusion when the reaction temperature $T \geqslant T_m/2$. In the case of Nb_3Sn and V_3Si the reaction temperatures are too low for bulk diffusion, but for V_3Ga which has a relatively low T_m of 1300°C the possibility of bulk diffusion exists. When bulk diffusion is rate-controlling, the models yield a parabolic growth,

$$R = k_4 t^{1/2}, \tag{12}$$

with

$$k_4 = \left(\frac{2D_\beta}{\bar{C}_\beta}(C_{\beta\alpha} - C_{\beta F})\right)^{1/2}, \tag{13}$$

where D_β is the bulk diffusivity of B atoms in the compound layer. Thus, the growth rate would increase with temperature. Most of the growth kinetic studies of V_3Ga have yielded a parabolic growth in support of this mechanism. However, $n = 0{\cdot}5$ can also result from grain boundary diffusion.

5.2b *Growth controlled by grain boundary diffusion*

(i) Zero grain growth. When the grain diameter d of the compound layer remains constant throughout diffusion reaction, the models again predict a parabolic growth

$$R = k_5 t^{1/2},$$

$$\text{with} \qquad k_5 = 2\left(\frac{aD_{gb}}{\alpha \bar{C}_\beta}(C_{\beta\alpha g} - C_{\beta F g})\right)^{1/2}, \tag{14}$$

where D_{gb} is the grain boundary diffusivity of B atoms in the compound layer. Since it increases with temperature, the layer growth is higher at elevated temperatures. $C_{\beta\alpha g}$ and $C_{\beta F g}$ are the Sn-concentrations in the boundary at the β-α and β-F interfaces. A higher Sn-concentration in the matrix provides a larger driving force for diffusion through boundaries by increasing $C_{\beta\alpha g} - C_{\beta F g}$ resulting in a faster layer growth. Further, R varies inversely as the square root of the grain diameter which corroborates the results of Togano *et al* (1979) and Wu *et al* (1983) obtained for Nb_3Sn layer grown from Mg-doped bronze matrix. They found that addition of <0·5% Mg led to a considerable reduction in grain growth and grain size which explains the enhanced parabolic growth which they observed. Similar effect was observed by Sekine and Tachikawa (1979) after doping Nb cores with Hf which resulted in doubling of the layer growth with simultaneous reduction in grain growth. In fact, wherever the grain growth has been negligible and there is an enhanced parabolic growth, zero grain growth model seems to be the right choice.

(ii) *Grain growth superimposed on grain boundary diffusion*: Consider an arbitrary grain growth described by

$$d_t = d_i + Gt^m, \tag{15}$$

where d_i is the initial or nucleation grain diameter, d_t the grain diameter after diffusion annealing at a fixed temperature for a time t, G is a temperature-dependent coefficient and m is a numerical time exponent.

(a) Small initial grain size: When the initial grain size is small the models predict grain growth-dependent layer growth given by

$$R = k_6 t^{(1-m)/2}, \tag{16}$$

$$\text{with} \qquad k_6 = 2\left(\frac{aD_{gb}}{\bar{C}_\beta G(1-m)}(C_{\beta\alpha g} - C_{\beta F g})\right)^{1/2}. \tag{17}$$

As discussed earlier (17) explains the observed increase in growth rate with temperature and Sn-concentration.

Whenever the layer growth is subparabolic the above model is the only choice. A parabolic grain growth, i.e., $m = 0{\cdot}5$, yields $n = 0{\cdot}25$. For grain growth slower than parabolic the n values will be intermediate between 0·25 and 0·5. When the grain growth is faster than parabolic n is expected to be <0·25. Thus the model explains the observed n values in subparabolic range reported in the literature. In general, a higher grain growth is expected at higher temperatures and the resulting n values are thus expected to decrease. This is consistent with the results of Larbalestier *et al* (1975) for Nb_3Sn, and Critchlow *et al* (1974) and Tachikawa *et al* (1972) obtained for V_3Ga. By careful transmission electron microscopic studies of grain growth and scanning electron microscopic studies of layer growth the interrelation between the layer growth kinetics and the grain growth kinetics has been experimentally confirmed (figure 7) by Agarwal and Narlikar (1985a).

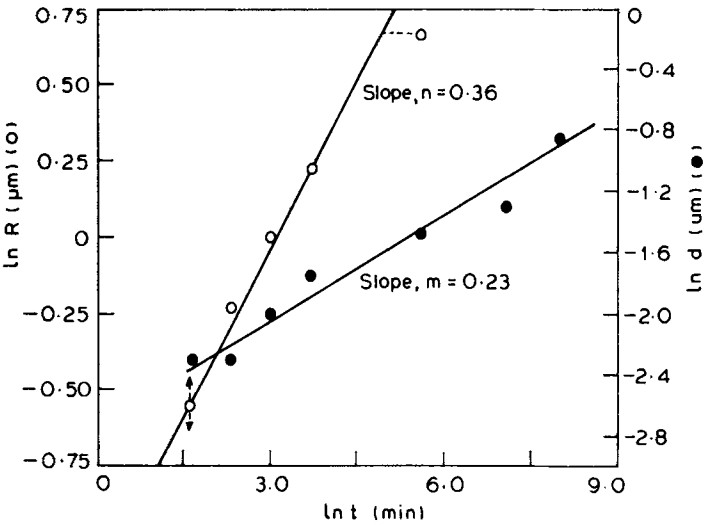

Figure 7. Interdependence of layer growth kinetics on grain growth kinetics (after Agarwal and Narlikar 1985a).

It is clear from (16) and (17) that the kinetics of layer growth can respond in a complicated way to various rate-controlling parameters. When the time exponent of layer growth $(1-m)/2$ is enhanced (due to decrease in temperature), k_6 is reduced by a factor $(1-m)$. Moreover, when the reaction temperature is lowered D_{gb} and G are expected to become smaller. Thus, the net increase or decrease of the layer growth with temperature would be determined by the overall effects of the above factors.

(b) *Large initial grain size*: When the initial grain size is large further grain growth is expected to have relatively less effect in reducing the grain boundary channels for diffusion. The situation, in effect, becomes analogous to that of zero grain growth described earlier. As expected, the growth law is parabolic

$$R = k_7 t^{1/2},$$

with

$$k_7 = 2\left(\frac{aD_{gb}}{d_i \bar{C}_\beta}(C_{\beta\alpha g} - C_{\beta F g})\right)^{1/2}, \tag{18}$$

which again shows that the growth rate would increase with temperature and the Sn-concentration in the matrix. Reaction rate constant decreases with increase in d_i. As already discussed in §3 the nucleation grain size increases with temperature, and consequently if the grain growth is small it is expected that the n values will gradually approach 0·5 as the reaction temperature is raised. Moreover, since $k_7 \propto d_i^{-1/2}$, and if the temperature dependence of d_i is more pronounced than D_{gb}, a decrease in the reaction rate constant would accompany increase in n as the reaction temperature is raised. These contentions have been substantiated by growth kinetic studies of Upadhyay *et al* (1981) (figure 8) and Agarwal *et al* (1984) on multifilamentary Nb_3Sn samples (figure 9). This mechanism can explain the parabolic growth frequently exhibited by V_3Ga. The grain size of V_3Ga layers is found to be two or three times larger than Nb_3Sn layers and consequently the time exponent for the growth of V_3Ga layer is expected to approach 0·5.

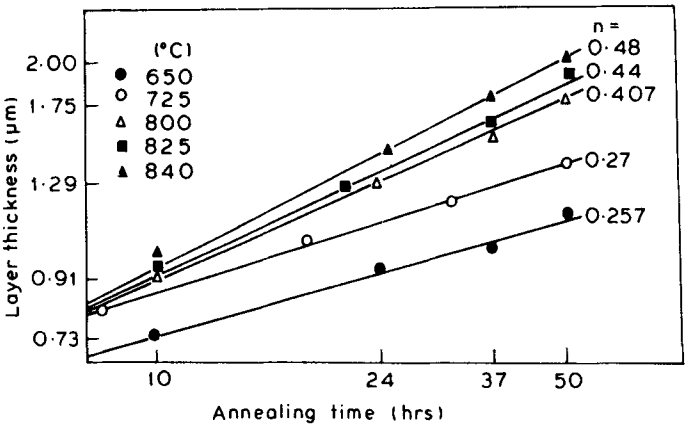

Figure 8. ln R vs ln t plots at different temperatures for Nb_3Sn layers (after Upadhyay *et al* 1981).

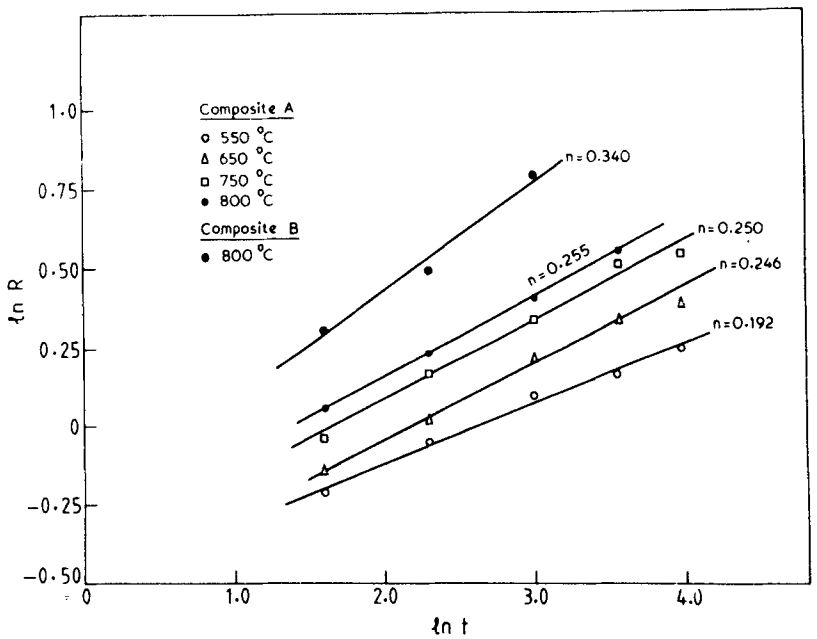

Figure 9. ln R vs ln t plots showing increase in n with reaction temperature (after Agarwal *et al* 1984).

6. Ordering kinetics

By ordering is meant the right species of atoms occupying the right crystallographic lattice sites. The LRO is measured by Bragg-Williams order parameter S, such that $S = 1$ when the compound is fully ordered and $S = 0$ when it is completely disordered. In the case of A-15 superconductors the critical temperature T_c depends sensitively on LRO and the ratio $T_c/T_{c(0)}$ serves as a satisfactory measure of S, where $T_{c(0)}$ is the optimum T_c value corresponding to $S = 1$.

Although the annealing-induced reordering of bulk A-15s, initially disordered by neutron irradiation or rapid quenching, has been studied fairly extensively, there are little data available to date on the ordering effects in A-15 layers formed by solid state diffusion. X-ray diffraction studies of Okuda *et al* (1983) have shown that the layers reacted at lower temperatures have lower T_c, are less ordered and are slightly tin-deficient than those formed at higher temperatures, and contain antisite defects. The kinetics of ordering as the compound layer starts growing has remained mostly unexplored to date. In contrast to the layer growth kinetics where the bulk or grain boundary diffusion are both possible, the ordering kinetics are governed only by bulk diffusion.

It is worthwhile to examine the problem of ordering kinetics of A-15 layers from the viewpoint of a simple diffusion process and also to consider the reordering kinetic models developed for bulk materials.

6.1 *Analytical models*

(i) Simple diffusion process

The process is simply vacancy filling by the right species of atoms, i.e. Sn atoms moving into vacant Sn sites and Nb into vacant Nb sites. The grains formed initially after the start of diffusion reaction are Nb-rich with excess Sn vacancies with surplus Sn concentration in the boundary region (Suenaga and Jansen 1983). In the first instance an increase in T_c with annealing can be attributed to the gradual filling up of Sn vacancies by flux of Sn atoms coming from the grain boundary region whereby the Sn concentration C within the grains is raised to the stoichiometric level. The process leads to

$$0{\cdot}25 - C = (0{\cdot}25 - C_i) \exp(-t/\tau), \tag{19}$$

which may be related directly to T_c,

$$T_{c(0)} - T_c = [T_{c(0)} - T_{ci}] \exp(-t/\tau), \tag{20}$$

where T_{ci} is T_c at $t = 0$, τ is the relaxation time for filling up of vacancies, related to the bulk diffusivity of Sn in the compound layer, and $C = C_i$ is the Sn concentration at $t = 0$. C_i and T_{ci} are attributed to the compound formed during intermittent annealings while wire drawing. If the above process were solely responsible for the observed T_c increase one should obtain the same relaxation time independently from Sn concentration and T_c data. Any substantial deviation would mean the presence of antisite disorders occurring as precurser to the final ordering.

(ii) Reordering kinetic models

Following Welch (unpublished), Dew-Hughes (1980) developed reordering kinetic models to explain the observed increase in T_c of disordered bulk materials after annealing in terms of vacancy assisted hopping of atoms from wrong lattice sites to the correct ones, and the rate of ordering is determined by the slower of the two species. Accordingly, when Sn atoms are slower than Nb atoms, the rate of ordering is governed by first order kinetics, giving

$$\ln \xi = \ln \xi_0 - 16 f_{v_0} \nu_B \exp[-U_{R(B)}/kT]\, t, \tag{21}$$

for t-small, and

$$\ln\xi = \ln\xi_0 - 16 V_0 \nu_B \exp[-\{U_{R(B)} + U_f\}/kT]t, \tag{22}$$

for t-large. When Sn atoms are faster than Nb atoms the kinetics is of second order, given by

$$\frac{1}{\xi} = \frac{1}{\xi_0} + 12 f_{v_0} \nu_A \exp[-U_{R(A)}/kT]t, \tag{23}$$

for t small, and

$$\frac{1}{\xi} = \frac{1}{\xi_0} + 12 V_0 \nu_A \exp[-\{U_{R(A)} + U_f\}/kT]t, \tag{24}$$

for t-large. $\xi = 1 - T_c/T_{c(0)}$ is a measure of order. $U_{R(A)}$ and $U_{R(B)}$ are the activation energies for reordering of Nb and Sn atoms respectively with ν_A and ν_B their attempt frequencies, and

$$f_v = f_{v_0} \exp(t/\tau) + V_0 \exp(-U_f/kT), \tag{25}$$

where f_{v_0} is the vacancy concentration in excess of the equilibrium value is associated with the vacancy formation energy U_f.

Experimental results of Winkel and Bakker (1985) on bulk samples of V_3Ga and the theoretical analysis of Nb_3Sn by Welch *et al* (1984) have indicated that while the grain boundary diffusivities of Ga and Sn are dominant in these systems their bulk diffusivities are respectively smaller than of V and Nb. Consequently, they attribute the ordering to be governed by first order kinetics.

Figure 10 depicts the results of Agarwal and Narlikar (1985b) showing the time dependence of T_c of Nb_3Sn layer formed after short durations of diffusion reaction. Long annealing times are of little use to understand ordering as the outermost grains of a layer formed in the beginning have already attained a near optimum T_c and the measuring techniques are not sensitive enough to record T_c increase due to subsequent ordering of inner grains. By measuring the lattice parameter and estimating the Sn concentration in the layer, Agarwal *et al* (1986) have found that the relaxation time obtained from (19) are over 30% smaller than determined from T_c data using (20). This rules out the simple diffusion process to be responsible for the observed T_c increase. On the other hand, if one considers the first order kinetics process operating over the whole time domain under study given by (21) and (22) a comparison of the slopes of $\ln\xi$ vs t plots (figure 11) yields a negative value of U_f which is clearly inconsistent. Similarly, attributing the observed change in the slope of $1/\xi$ vs t at $t \simeq 400$ sec to t-small and t-large of (23) and (24) of second order kinetics is also unrealistic since the relaxation times involved are two or three times larger. Agarwal *et al* (1986) instead find that the observed data can be best explained by a duplex process. Initially the kinetics is of second order and subsequently changing over to first order. $U_{R(A)}$ and $U_{R(B)}$ are found to be 1·46 and 1·13 eV respectively, which are consistent with the values reported by Dew Hughes (1980).

The above findings are of course preliminary and need to be further substantiated by more data on other systems. Unfortunately, relatively little is known about the

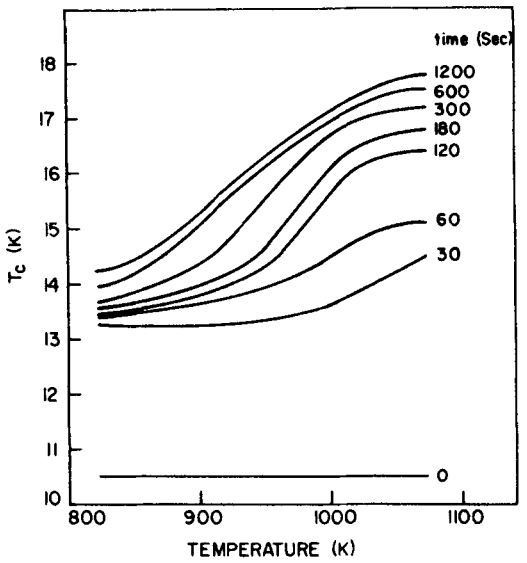

Figure 10. Time dependence of T_c of Nb_3Sn formed after short durations of reaction (after Agarwal and Narlikar 1985b).

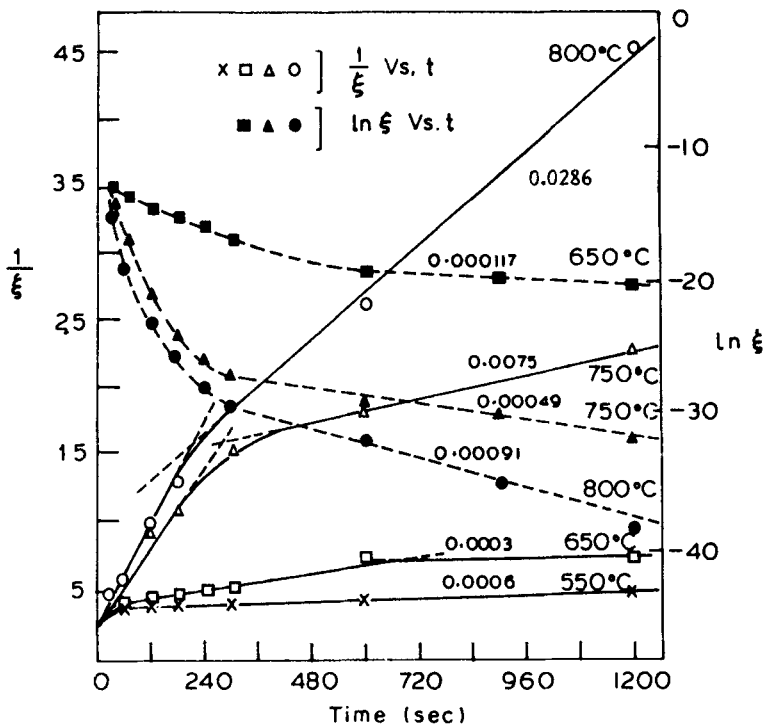

Figure 11. Plot of various ordering mechanisms (after Agarwal *et al* 1986).

behaviour of point defects in A-15s, in fact, in intermetallics in general, and the theoretical analysis of Welch *et al* (1984) has indicated it to be much more complex than known for pure metals. According to Welch (1985) the reordering kinetic models need a considerable refinement to become more realistic.

7. Conclusions

The story of transformation kinetics of A-15 formation may be summed up by making following broad observations.

To start with, we do not seem to have any relevant data relating to how the nucleation of the A-15 phase takes place in the diffusion couple. The problem is discussed in a general way, making some obvious predictions which seem to have experimental confirmation. Regarding the grain structure of A-15 layers considerable information is available about grain morphology and its dependence on process parameters, but on the grain growth aspect the situation is bleak. Presence of rather small grain sizes necessitates the use of transmission electron microscopy technique where the sample preparation of multifilamentary composites is an art mastered by a few. In lieu of adequate knowledge of grain growth data there is little choice left but to make some speculative assumptions pertaining to grain growth in order to explain the observed data on layer growth. The present knowledge of layer growth kinetics is however on a firm footing. The variation of growth laws seem explicable by model calculations compatible with the process conditions. A few gaps in the story still remain: one already mentioned above, i.e., the grain growth kinetics, and the second, the role of impurities. An unequivocal understanding of the effect of impurities on the layer growth kinetics is yet to emerge. There are no clear guidelines available about which one must add impurities or alloying elements to the diffusion couple to accelerate the layer growth. This would have an immediate relevance to the optimization of properties. The area of ordering kinetics is a new and growing area. Recent theoretical studies have indicated it to be a rich field involving unusual behaviour of point defects. Likewise, preliminary experimental findings of ordering kinetics of growing Nb_3Sn layers pose exciting challenges calling for further work.

References

Agarwal S K, Samanta S B, Batra V K and Narlikar A V 1984 *J. Mater. Sci.* **19** 2057
Agarwal S K and Narlikar A V 1985a *Proc. Int. Conf. Cryogenics (Calcutta)* in press
Agarwal S K and Narlikar A V 1985b *Solid State Commun.* **55** 563
Agarwal S K, Nagpal K C and Narlikar A V 1986 *Solid State Commun.* **58** 89
Berthel K H, Fischer K, Fuchs G, Grunberger W, Holzhauseer W, Lange F, Rohr S and Schumann H J 1978 *Proc. VI Int. Conf. Magnet-Technology ALFA*, p. 1007
Cahn J and Hagel W 1962 *Decomposition of austenite by diffusion process* (eds) V Zackay and H Aaronson (New York: Interscience) p. 134
Cave J R and Weir C A 1983 *IEEE Trans. Magnetics* **MAG-19** 1120
Critchlow P R, Gregory E and Marancik W 1974 *J. Appl. Phys.* **45** 5027
Dew-Hughes D 1980 *J. Phys. Chem. Solids* **41** 851
Dew-Hughes D, Luhman T S and Suenaga M 1976 *Nucl. Technol.* **29** 268
Dew-Hughes D and Luhman T S 1978 *J. Mater. Sci.* **13** 1868
Dew-Hughes D and Suenaga M 1978 *J. Appl. Phys.* **49** 357

Larblestier D C, Madsen P F, Lee J A, Wilson M N and Harlesworth J P 1975 *IEEE Trans. Mag.* **11** 247
Livingston J D 1977 *J. Mater. Sci.* **12** 1759
Luhamn T S and Suenaga M 1977 *Adv. Cryog. Engg.* **22** 356
Narlikar A V and Dew-Hughes D 1985a *Fabrication techniques for A-15 compound superconductors* (ed.) D Dew-Hughes (Amsterdam: North Holland) to be published
Narlikar A V and Dew-Hughes D 1985b *Proc. Int. Conf. Cryogenics (Calcutta)* in press
Okuda S, Suenaga M and Sabatini R L 1983 *J. Appl. Phys.* **54** 289
Reddi B V, Ray S, Raghavan V and Narlikar A V 1978 *Philos. Mag.* **A38** 559
Reddi B V, Raghavan V, Ray S and Narlikar A V 1983 *J. Mater. Sci.* **18** 1165
Sekine H and Tachikawa K 1979 *Appl. Phys. Lett.* **35** 472
Suenaga M, Horigami O and Luhman T S 1974 *Appl. Phys. Lett.* **25** 624
Suenaga M 1981 *Superconductor materials sciences* (eds) S Foner and B B Schawartz (New York: Plenum) p. 201
Suenaga M and Jansen 1983 *Appl. Phys. Lett.* **43** 791
Tachikawa K, Yoshida Y and Rinderer L 1972 *J. Mater. Sci.* **7** 1154
Togano K, Asan T and Tachikawa K 1979 *J. Less Common Metals* **68** 15
Upadhyay P, Samanta S B and Narlikar A V 1981 *Mater. Res. Bull.* **16** 741
Wada H, Kimura M and Tachikawa K 1978 *J. Mater. Sci.* **13** 1943
Welch D O, Diences G J, Lazareth O W Jr and Hatcher R D 1984 *J. Phys. Chem. Solids* **45** 1125
Welch D O 1985 Private Communication
Winkel A V and Bakker H 1985 *J. Phys.* **F15** 1556
Wu I W, Dietderich D R, Hottuis W V and Morris J W Jr 1983 *IEEE Trans. Magnetics* **MAG-19** 1437